

# New Push–Pull Dyes Derived from Michler's Ketone For Polymerization Reactions Upon Visible Lights.

Mohamad-Ali Tehfe,<sup>†</sup> Frédéric Dumur,<sup>‡</sup> Bernadette Graff,<sup>†</sup> Fabrice Morlet-Savary,<sup>†</sup> Jean-Pierre Fouassier,<sup>§</sup> Didier Gigmes,<sup>\*,‡</sup> and Jacques Lalevée<sup>\*,†</sup>

<sup>†</sup>Institut de Science des Matériaux de Mulhouse IS2M – UMR CNRS 7361 – UHA; 15, rue Jean Starcky, 68057 Mulhouse Cedex – France

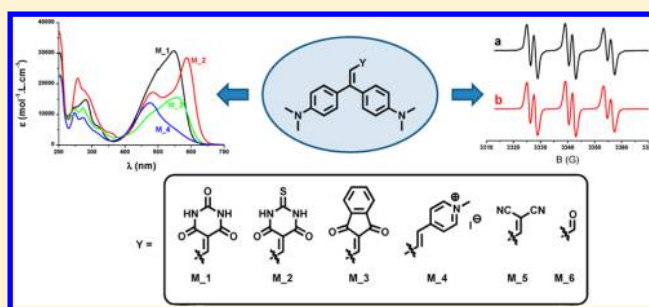
<sup>‡</sup>Aix-Marseille Université, CNRS, Institut de Chimie Radicalaire, UMR 7273, F-13397 Marseille, Cedex 20, France

<sup>§</sup>UHA-ENSCMu, 3 rue Alfred Werner, 68093 Mulhouse, France

## Supporting Information

**ABSTRACT:** Among other photoinitiating systems, aromatic ketone based compounds have been largely exploited as photoinitiators (PIs). However, none of these compounds efficiently absorb above 420 nm. The search of novel architectures of PIs for getting an important red-shift of the absorption is crucial for the use of visible lights for polymer synthesis. Novel bifunctional dyes derived from the Michler's ketone structure are proposed here as photoinitiators for the free radical polymerization of acrylates and the cationic polymerization of epoxides upon exposure to 457, 473, and 532 nm laser diodes and even to a green LED bulb at 514 nm.

Excellent polymerization profiles are obtained. These original dyes exhibit a push–pull molecular character for a remarkable covering of the visible lights. The formation of the radicals and the ions in the two- and three-component photoinitiating systems is described and the initiation steps are discussed.



## INTRODUCTION

The development of photoinitiators PI of polymerization is an attractive research field (see e.g. in<sup>1,2</sup>). Among other PI systems, aromatic (and aliphatic to a lesser extent) ketone based compounds (benzophenones, thioxanones, anthraquinones, fluorenones, ketocoumarines, camphorquinones...) have been largely exploited as photoinitiators. Benzophenone BP, originally one of the model molecule for photochemists,<sup>3</sup> has been undoubtedly considered all along the years as an interesting starting structure (and presumably the most widely used) where structural modifications can be easily introduced to improve the absorption properties or the photochemical reactivity. Benzophenone is a Type II PI working through electron/proton transfer or hydrogen abstraction. A huge number of Type II BP derivatives have been synthesized and studied. They involved (i) compounds bearing somewhat usual substituents<sup>4</sup> linked by a carbon atom (alkyl, phenyl, benzoyl, trimethylsilyl, acrylate, ...), an oxygen (alkoxy, phenoxy, ...), a sulfur (thioether...), or a nitrogen (4,4'-dimethylaminobenzophenone or Michler's ketone MK, 4,4'-diethylaminobenzophenone EAB...), (ii) water-soluble derivatives,<sup>5</sup> (iii) slightly modified skeletons,<sup>6</sup> oligomeric or polymeric arrangements,<sup>7</sup> and tailor-made two-photon absorbing compounds.<sup>8</sup> Type I cleavable benzophenone derivatives (that can also behave as Type I PIs) have been developed;<sup>9</sup> they contain, e.g., a sulfoxide, a thiobenzoate, a phenyl sulfide, a sulfonyl (BPSK), a

tris(trimethylsilyl) silyloxy (BP–OSi), an alkoxyamine (BP–N(X)–Y) or a *N*-phenylglycine moiety, several preester groups...

The one-photon  $\pi$ – $\pi^*$  absorption properties of most of these benzophenone derivatives remain close to that of BP itself ( $\lambda_{\text{max}} \sim 250$  nm,  $\epsilon_{\text{max}} = 18700$  M<sup>-1</sup> cm<sup>-1</sup>; forbidden n– $\pi^*$  transition at  $\sim 350$  nm,  $\epsilon_{\text{max}} = 200$  M<sup>-1</sup> cm<sup>-1</sup>), the best red-shifts being typically observed for MK or EAB ( $\lambda_{\text{max}} \sim 365$  nm,  $\epsilon_{\text{max}} = 44000$  M<sup>-1</sup> cm<sup>-1</sup> in acetonitrile), BPSK ( $\lambda_{\text{max}} \sim 313$  nm,  $\epsilon_{\text{max}} = 18900$  M<sup>-1</sup> cm<sup>-1</sup>), BMS ( $\lambda_{\text{max}} \sim 310$  nm,  $\epsilon_{\text{max}} = 18200$  M<sup>-1</sup> cm<sup>-1</sup>) or BP–OSi (no clear absorption maximum is observed at  $\lambda > 300$  nm despite extinction coefficients higher than for benzophenone;  $\epsilon_{350 \text{ nm}} \sim 400$  M<sup>-1</sup> cm<sup>-1</sup>). None of these compounds efficiently absorb above 420 nm.

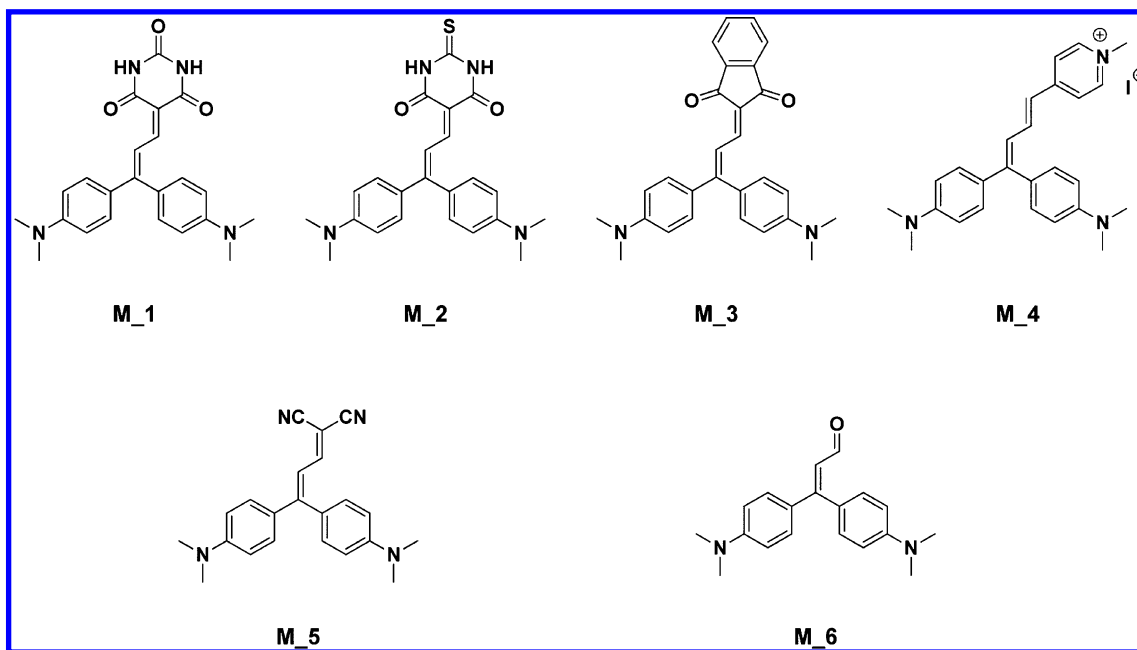
In the frame of our recent works devoted to the design of highly absorbing PIs in the visible wavelength range through the search of novel architectures of modified existing PIs or di- and trifunctional PIs,<sup>10</sup> we look for another new way for getting a more important red-shift of the absorption of BP related compounds. Indeed, usual electron delocalization cannot ensure important modifications in the ground state absorption spectra. On the opposite, as known in photochemistry,

Received: April 13, 2013

Revised: April 29, 2013

Published: May 14, 2013

Scheme 1



introducing push–pull effects in the coupled moieties of di- or trifunctional compounds allows dramatic changes in the absorption through a substantial charge transfer CT: this property was recently used for the design of blue to yellow, blue to green or blue to red photosensitive systems.<sup>11</sup> We explore here structurally related Michler's ketone derivatives allowing the use of true visible light irradiation sources. In the present paper, novel Ar–(C=C–Y)–Ar bifunctional dye structures where Y stands for a barbituric, a thiobarbituric, an indanedione, a pyridinium, a dicyanovinyl, or an aldehyde moiety are proposed (Scheme 1). They can be considered as a Michler's ketone (Ar–(C=O)–Ar) derivative where the C=O bond is changed for a C=C–Y moiety. The use of these dyes in two- and three-component photoinitiating systems for the free radical polymerization of acrylates and the cationic polymerization of epoxides upon exposure to 457, 473, and 532 nm laser diodes and even to a green LED bulb at 514 nm is studied. The formation of the radicals and the ions in two- and three-component photoinitiating systems is described and the initiation steps are also discussed.

## EXPERIMENTAL SECTION

**i. Synthesis of the Different Dyes.** All reagents and solvents were purchased from Aldrich or Alfa Aesar and used as received without further purification. Mass spectroscopy was performed by the Spectropole of Aix-Marseille University. ESI mass spectral analyses were recorded with a 3200 QTRAP (Applied Biosystems SCIEX) mass spectrometer. The HRMS mass spectral analysis was performed with a QStar Elite (Applied Biosystems SCIEX) mass spectrometer. Elemental analyses were recorded with a Thermo Finnigan EA 1112 elemental analysis apparatus driven by the Eager 300 software. <sup>1</sup>H and <sup>13</sup>C NMR spectra were determined at room temperature in 5 mm o.d. tubes on a Bruker Avance 400 spectrometer of the Spectropole: <sup>1</sup>H (400 MHz) and <sup>13</sup>C (100 MHz). The <sup>1</sup>H chemical shifts were referenced to the solvent peak DMSO-*d*<sub>6</sub> (2.49 ppm), CDCl<sub>3</sub> (7.26 ppm) and the <sup>13</sup>C chemical shifts were referenced to the solvent peak DMSO-*d*<sub>6</sub> (39.5 ppm), CDCl<sub>3</sub> (77 ppm). 3,3-Bis(4-(dimethylamino)phenyl)acrylaldehyde **M\_6** (Michler's aldehyde)<sup>12</sup> and **M\_4** were synthesized as previously reported.<sup>13</sup> Synthesis of 2-(3,3-bis(4-(dimethylamino)phenyl)allylidene)malononitrile **M\_5** was previously

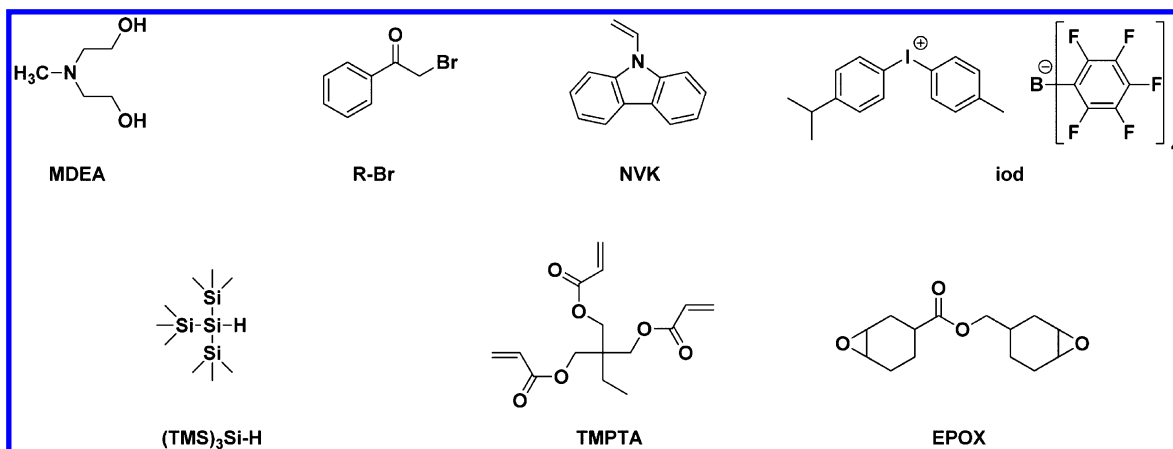
reported in the literature, in other Knoevenagel conditions and in lower yield.<sup>14</sup> The three dyes **M\_1–M\_3** were prepared by Knoevenagel condensation of 3,3-bis(4-(dimethylamino)phenyl)acrylaldehyde with the corresponding electron acceptor.

**Synthesis of 5-(3,3-Bis(4-(dimethylamino)phenyl)allylidene)pyrimidine-2,4,6(1H,3H,5H)-trione, M\_1.** Michler's aldehyde (1 g, 3.40 mmol) and barbituric acid (0.43 g, 3.40 mmol) were dissolved in absolute ethanol (20 mL). A few drops of piperidine were added. Immediately, the solution turned indigo. The solution was refluxed for 4 h. After cooling, the solvent was removed under reduced pressure. Addition of chloroform followed by pentane precipitated a black solid, which was filtered off, washed several times with pentane, and dried under vacuum. The title molecule was obtained in 84% yield (1.15 g) <sup>1</sup>H NMR (CDCl<sub>3</sub>), δ (ppm): 3.08 (s, 12H), 6.66 (d, 2H, *J* = 8.9 Hz), 6.74 (d, 2H, *J* = 8.9 Hz), 7.21 (d, 2H, *J* = 8.9 Hz), 7.45 (d, 2H, *J* = 8.9 Hz), 8.14 (d, 1H, *J* = 13.1 Hz), 8.32 (d, 1H, *J* = 13.1 Hz). <sup>1</sup>H NMR (DMSO-*d*<sub>6</sub>), δ (ppm): 3.04 (s, 12H), 6.78 (d, 2H, *J* = 9.1 Hz), 6.83 (d, 2H, *J* = 8.9 Hz), 7.10 (d, 2H, *J* = 8.8 Hz), 7.28 (d, 2H, *J* = 9.0 Hz), 7.85 (d, 1H, *J* = 12.8 Hz), 8.20 (d, 1H, *J* = 12.8 Hz). <sup>13</sup>C NMR (DMSO-*d*<sub>6</sub>), δ (ppm): 44.2, 109.7, 111.3, 111.7, 118.3, 124.5, 127.3, 131.8, 133.2, 150.4, 151.7, 152.3, 163.5, 164.0, 166.3; HRMS (ESI MS) *m/z*: theor, 404.1848; found, 404.1845 (*M*<sup>+</sup> detected).

**Synthesis of 5-(3,3-Bis(4-(dimethylamino)phenyl)allylidene)-2-thioxodihydropyrimidine-4,6(1H,5H)-dione, M\_2.** Michler's aldehyde (1 g, 3.40 mmol), thiobarbituric acid (0.49 g, 3.40 mmol) were dissolved in absolute ethanol (20 mL). A few drops of piperidine were added. Immediately, the solution turned dark violet. The solution was refluxed for 4 h. After cooling, the solvent was removed under reduced pressure. Addition of chloroform followed by pentane precipitated a solid which was filtered off, washed several times with pentane and dried under vacuum. The chromophore was obtained in 78% yield (1.11 g). <sup>1</sup>H NMR (CDCl<sub>3</sub>), δ (ppm): 3.10 (s, 6H), 3.11 (s, 6H), 6.66 (d, 2H, *J* = 8.9 Hz), 6.73 (d, 2H, *J* = 8.9 Hz), 7.21 (d, 2H, *J* = 8.8 Hz), 7.49 (d, 2H, *J* = 8.9 Hz), 8.09 (d, 1H, *J* = 13.3 Hz), 8.39 (d, 1H, *J* = 13.3 Hz). <sup>1</sup>H NMR (DMSO-*d*<sub>6</sub>), δ (ppm): 3.06 (s, 12H), 6.79–6.85 (m, 4H), 7.13 (d, 2H, *J* = 8.7 Hz), 7.32 (d, 2H, *J* = 8.9 Hz), 7.84 (d, 1H, *J* = 12.3 Hz), 8.24 (d, 1H, *J* = 12.3 Hz). <sup>13</sup>C NMR (DMSO-*d*<sub>6</sub>), δ (ppm): 44.8, 111.3, 111.41, 111.45, 111.8, 118.9, 124.5, 127.1, 132.4, 133.6, 152.0, 152.7, 163.6, 174.0, 177.7; HRMS (ESI MS) *m/z*: theor, 420.1620; found, 420.1622 (*M*<sup>+</sup> detected).

**Synthesis of 2-(3,3-Bis(4-(dimethylamino)phenyl)allylidene)-1H-indene-1,3(2H)-dione, M\_3.** Michler's aldehyde (1 g, 3.40 mmol) and indane-1,3-dione (0.49 g, 3.40 mmol) were dissolved in absolute

Scheme 2



ethanol (20 mL). Immediately, the solution turned deep red. The solution was refluxed for 4 h. After cooling, the solvent was removed under reduced pressure. Addition of a minimum of ether followed by pentane precipitated a deep green solid which was filtered off, washed several times with ether and dried under vacuum. The title chromophore was obtained in 72% yield (1.03 g).  $^1\text{H}$  NMR (DMSO- $d_6$ ),  $\delta$  (ppm): 3.06 (s, 6H), 3.07 (s, 6H), 6.66 (d, 2H,  $J = 8.9$  Hz), 6.76 (d, 2H,  $J = 8.7$  Hz), 7.20 (d, 2H,  $J = 8.7$  Hz), 7.45 (d, 2H,  $J = 8.9$  Hz), 7.67–6.72 (m, 3H), 7.83–7.86 (m, 2H), 8.29 (d, 1H,  $J = 12.7$  Hz).  $^{13}\text{C}$  NMR (DMSO- $d_6$ ),  $\delta$  (ppm): 40.1, 40.2, 111.40, 111.44, 118.7, 122.1, 122.3, 123.8, 125.6, 128.7, 132.2, 133.4, 133.6, 133.9, 134.1, 134.3, 140.6, 142.0, 145.5, 151.7, 152.1, 165.7, 191.4, 191.5; HRMS (ESI MS)  $m/z$ : theor, 422.1994; found, 422.1995 ( $\text{M}^+$  detected).

**Synthesis of 2-(3,3-Bis(4-(dimethylamino)phenyl)allylidene)malononitrile, M<sub>5</sub>.** Michler's aldehyde (1 g, 3.40 mmol) and malononitrile (0.22 g, 3.40 mmol) were dissolved in absolute ethanol (50 mL). A few drops of piperidine were added. Immediately, the solution turned deep red. The solution was refluxed for 2 h. After cooling, the solvent was removed under vacuum. Addition of a minimum of ether followed by pentane precipitated a Bordeaux-black solid which was filtered off and dried under vacuum. The chromophore was obtained in 95% yield (1.11 g).  $^1\text{H}$  NMR ( $\text{CDCl}_3$ ),  $\delta$  (ppm): 3.06 (s, 6H), 3.07 (s, 6H), 6.64 (d, 2H,  $J = 9.1$  Hz), 6.73 (d, 2H,  $J = 8.8$  Hz), 6.95 (d, 1H,  $J = 12.3$  Hz), 7.10 (d, 2H,  $J = 9.1$  Hz), 7.35 (d, 2H,  $J = 8.8$  Hz), 7.48 (d, 1H,  $J = 12.3$  Hz).  $^{13}\text{C}$  NMR ( $\text{CDCl}_3$ ),  $\delta$  (ppm): 40.1, 40.2, 74.5, 111.40, 111.44, 113.9, 116.1, 116.6, 125.0, 127.1, 132.1, 133.0, 151.8, 152.5, 159.1, 163.8; HRMS (ESI MS)  $m/z$ : theor, 343.1917; found, 343.1919 ( $[\text{M} + \text{H}]^+$  detected).

**ii. Chemical Compounds.** *N*-Methylethanolamine (MDEA), phenacyl bromide (R-Br), *N*-vinylcarbazole (NVK), and tris(trimethylsilyl)silane ( $(\text{TMS})_3\text{SiH}$ ) were obtained from Aldrich and used with the best purity available (Scheme 2). [Methyl-4 phenyl-(methyl-1-ethyl)-4-phenyl]iodonium tetrakis(pentafluorophenyl)-borate (Iod) was obtained from Bluestar Silicones-France. (3,4-Epoxycyclohexane)methyl 3,4-epoxycyclohexylcarboxylate (EPOX; Uvacure 1500) and trimethylolpropane triacrylate (TMPTA) were obtained from Cytec (Scheme 2). EPOX and TMPTA were selected as representative multifunctional monomers for cationic and radical polymerizations, respectively. The formation of polymer networks is expected.

**iii. Irradiation Sources.** Several lights were used: (i) Polychromatic light from a halogen lamp (Fiber-Lite, DC-950 - incident light intensity:  $I_0 \approx 12 \text{ mW cm}^{-2}$ ; in the 370–800 nm range); (ii) Monochromatic light delivered by laser diodes at 457, 473, and 532 nm (MBL-III-BFIOPTILAS;  $I_0 \approx 100 \text{ mW cm}^{-2}$ ). A laser diode at 405 nm was also used ( $I_0 \approx 12 \text{ mW cm}^{-2}$ ). The emission spectra of these laser beams are given in ref 15a. (iii) Green light (514 nm;  $\sim 15 \text{ mW/cm}^2$ ) emitted by a LED bulb already presented in ref 15b.

#### iv. Free Radical Photopolymerization (FRP) Experiments.

Trimethylolpropane triacrylate (TMPTA from Cytec) was used as a low viscosity monomer. The experiments were carried out in laminated conditions. The films (25  $\mu\text{m}$  thick) deposited on a  $\text{BaF}_2$  pellet were irradiated (see the irradiation sources). The evolution of the double bond content was continuously followed by real time FTIR spectroscopy (JASCO FTIR 4100) at about  $1630 \text{ cm}^{-1}$  as in ref 16.

**v. Cationic Polymerization (CP) and Free Radical Promoted Cationic Polymerization (FRPCP).** The two- and three-component photoinitiating systems are based on dye/iodonium salt (0.3%/2% w/w) and dye/iodonium salt/NVK (0.3%/2%/3% w/w), respectively. The experimental conditions are given in the figure captions. The residual weight content is related to the monomer. The photosensitive formulations (25  $\mu\text{m}$  thick) were deposited on a  $\text{BaF}_2$  pellet under air. The evolution of the epoxy group content was continuously followed by real time FTIR spectroscopy (JASCO FTIR 4100) at about  $790 \text{ cm}^{-1}$ , respectively.<sup>16</sup>

**vi. Computational Procedure.** Molecular orbital calculations were carried out with the Gaussian 03 suite of programs. The electronic absorption spectra for the different compounds were calculated with the time-dependent density functional theory at B3LYP/6-31G\* level on the relaxed geometries calculated at UB3LYP/6-31G\* level.<sup>17</sup>

**vii. ESR Spin Trapping (ESR-ST) Experiments.** The ESR-ST experiments were carried out using an X-Band spectrometer (MS 400 Magnetech). The radicals were produced at RT under a halogen lamp exposure under  $\text{N}_2$  and trapped by phenyl-*N*-tert-butyl nitron (PBN) according to a procedure described in detail in ref 18. The ESR spectra simulations were carried out with the PEST WINSIM program.

**viii. Fluorescence Experiments.** The fluorescence properties of the compounds were studied using a JASCO FP-750 spectrometer.

**ix. Redox Potentials.** The redox potentials were measured in acetonitrile by cyclic voltammetry with tetrabutyl-ammonium hexafluorophosphate 0.1 M as a supporting electrolyte. The free energy change  $\Delta G_{\text{et}}$  for an electron transfer reaction is calculated from the classical Rehm–Weller equation (eq 1)<sup>19</sup> where  $E_{\text{ox}}$ ,  $E_{\text{red}}$ ,  $E_{\text{S}}$ , and  $C$  are the oxidation potential of the donor, the reduction potential of the acceptor, the excited state energy and the Coulombic term for the initially formed ion pair, respectively.  $C$  is neglected as is usually done in polar solvents.<sup>20</sup>

$$\Delta G_{\text{et}} = E_{\text{OX}} - E_{\text{red}} - E_{\text{S}} + C \quad (1)$$

**x. Laser Flash Photolysis.** Nanosecond laser flash photolysis (LFP) experiments were carried out using a Q-switched nanosecond Nd/YAG laser ( $\lambda_{\text{exc}} = 355 \text{ nm}$ , 9 ns pulses; energy reduced down to 10 mJ) from Continuum (Minilite) and an analyzing system consisting of a ceramic xenon lamp, a monochromator, a fast photomultiplier and a transient digitizer (Luzchem LFP 212).<sup>10</sup>

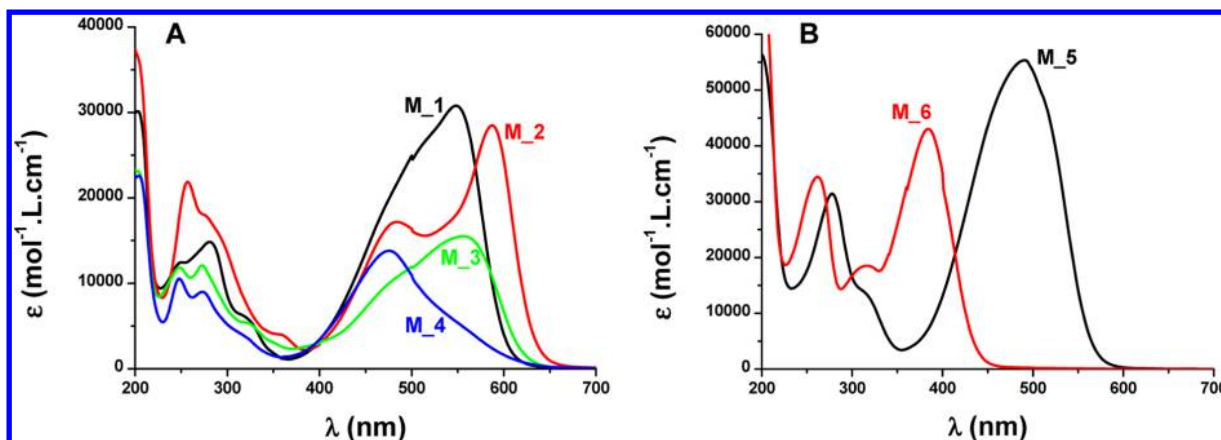


Figure 1. UV–visible absorption spectra of (A)  $M_1$ ,  $M_2$ ,  $M_3$ ,  $M_4$  and (B)  $M_5$ ,  $M_6$  in acetonitrile.

## RESULTS AND DISCUSSION

**1. Absorption Properties of the New Dyes.** The ground state absorption spectra of the proposed dyes (Figure 1) allow a large and efficient matching with the various visible light sources (halogen lamp and laser diodes at 405, 457, 473, and 532 nm). Remarkably, high molar extinction coefficients are determined for a green light, e.g.,  $\sim 28\,500$ ,  $16\,200$ ,  $14\,400$ ,  $7000$ , and  $32\,750\text{ M}^{-1}\text{ cm}^{-1}$ , for  $M_1$ ,  $M_2$ ,  $M_3$ ,  $M_4$ , and  $M_5$ , respectively at  $\sim 532\text{ nm}$ . These visible light absorptions can be advantageously compared to that of the classical Michler's ketone (see the Introduction). For  $M_6$ , the absorption is red-shifted compared to the Michler ketone MK ( $\lambda_{\text{max}} = 385\text{ nm}$  vs  $365\text{ nm}$ ) but the visible light absorption remains weak, i.e.,  $\epsilon_{450\text{ nm}} \sim 1000\text{ M}^{-1}\text{ cm}^{-1}$ .

These dyes can be considered as push–pull aromatic chromophores. The unsymmetrically substituted D– $\pi$ –A arrangements bearing electron donor (D) and electron acceptor (A) functionalities at both ends of a planar conjugated spacer are well-known to feature a large change in their absorption spectra and/or emission spectra as a function of the solvent polarity and the respective strength of the electron releasing and electron withdrawing groups.

Molecular orbital MO calculations (using the time-dependent density functional theory at B3LYP/6-31G\* level on the relaxed geometries calculated at UB3LYP/6-31G\* level) show that the lowest energy transition (that exhibits a  $\pi \rightarrow \pi^*$  character) involves strongly delocalized highest occupied molecular orbitals (HOMO) and lowest unoccupied molecular orbitals (LUMO) for all the investigated new dyes (Figure 2).

For  $M_1$  to  $M_3$  and  $M_5$  and  $M_6$ , the HOMO and LUMO are mainly localized on the donor (dimethylamino phenyl moiety) and the acceptor (barbituric for  $M_1$ , thiobarbituric for  $M_2$ , indanedione for  $M_3$ , dicyanovinyl for  $M_5$ , or aldehyde for  $M_6$ ) fragment, respectively. This highlights a charge transfer character in agreement with a push–pull structure (Figure 2). For  $M_4$ , the situation is different as the HOMO and LUMO are localized on the pyridinium moiety (Figure 2).

A solvatochromic study was carried out for  $M_1$ , this compound being characterized by the highest efficiency in the associated photoinitiating systems (see below). The maximum absorption wavelengths in different solvents are gathered in Table 1. The important Stoke shifts confirm the charge transfer character of the transition. No direct relationships were found with the empirical solvatochromic scales evidencing a behavior

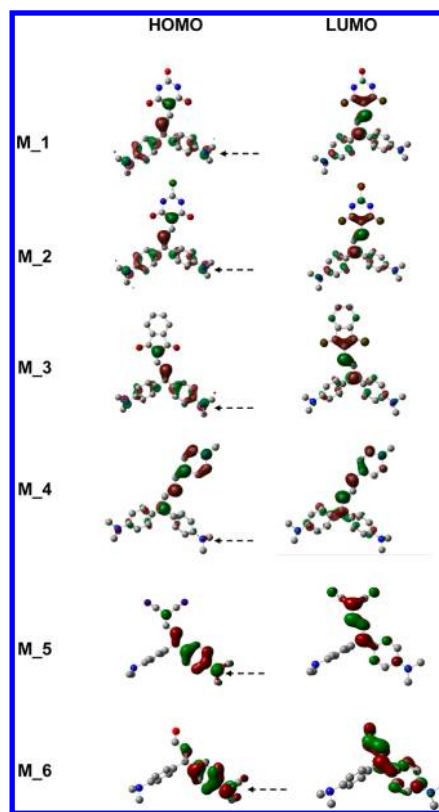


Figure 2. Molecular orbitals (HOMO (left) and LUMO (right)) for  $M_1$  to  $M_6$  (at UB3LYP/6-31G\* level); the dimethyl amino group is indicated by an arrow; the hydrogens are not depicted.

more complex than that recently encountered in other proposed push–pull systems.<sup>11</sup>

**2. Cationic Photopolymerization of EPOX.** The best typical conversion–time profiles of an epoxy monomer (EPOX) under air upon visible lights (laser diode irradiations at 457, 473, or 532 nm; green LED bulb at 514 nm; halogen lamp) are shown in Figures 3 and 4. Quite slow conversions are obtained with the dye/Iod initiating systems (e.g., Figure 3 curve 1). The presence of NVK drastically improves the polymerization profiles (e.g., Figure 3 curve 1 vs curve 2). NVK only absorbs in the UV range and can not be used as a photosensitizer upon visible light i.e. the two-component system NVK/Iod is not efficient for polymerization upon laser diode. The dye is required for an efficient sensitization

**Table 1.** Absorption and Emission Maxima (nm) of **M\_1** Measured by UV–Visible Spectroscopy and Fluorescence Spectroscopy

solvent	dielectric constant ( $\epsilon$ )	refractive index ( $n$ )	$\lambda_{\text{max}}$ ( <b>M_1</b> )	$\lambda_{\text{em}}$ ( <b>M_1</b> )	Stoke shift
<i>tert</i> -butylbenzene	2.3	1.493	540	582	42
toluene	2.4	1.497	542	588	46
chloroform	4.8	1.446	567	598	31
THF	7.4	1.407	526	584	58
CH <sub>2</sub> Cl <sub>2</sub>	8.9	1.424	563	600	37
acetone	20.6	1.359	537	n.e. <sup>a</sup>	–
methanol	32.7	1.328	561	599	38
acetonitrile	37.5	1.344	548	600	52
water	–	–	581	n.e.	–
([acetonitrile] = 0.2 M)					

<sup>a</sup>n.e.: non-evaluated (too weak to be measured).

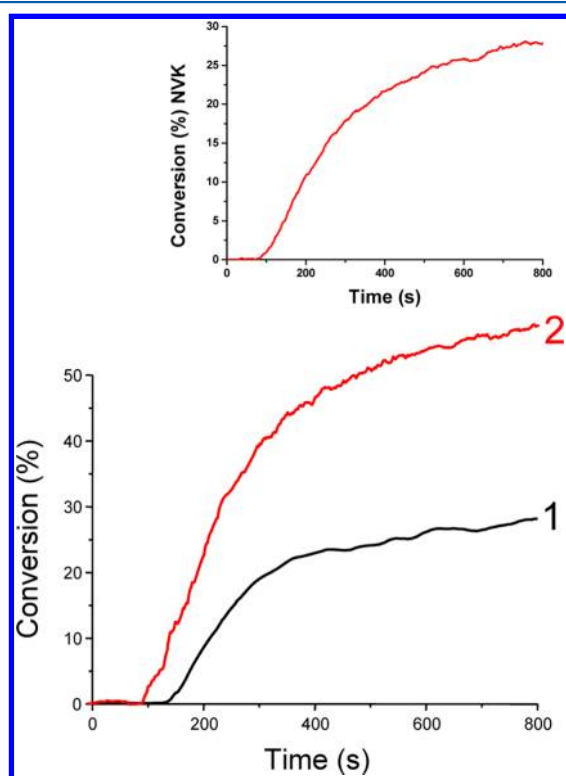


**Figure 3.** Photopolymerization profiles of EPOX under air upon a laser diode exposure at 532 nm in the presence of (1) **M\_1**/Iod (0.3%/2% w/w) or (2) **M\_1**/NVK/Iod (0.3%/3%/2% w/w); Inset: conversion of NVK for run 2.

process. The dye efficiency follows the **M\_1** > **M\_3** > **M\_2** ~ **M\_5** > **M\_6** series (Figure 4A); i.e., **M\_4** is not stable in presence of the iodonium salt, leading to a degradation of the sample: this latter compound will not be investigated further. MK itself does not work under such conditions. **M\_6** does not work at 532 nm (i.e., this compound does not absorb for this wavelength) but can be used for halogen lamp or 405 nm laser diode irradiations (final conversions >40% can be reached using **M\_6**/Iod/NVK).

**M\_1** being the most reactive, its associated polymerization initiating ability was investigated upon different laser diode irradiations (457, 473, and 532 nm; Figure 4B; tack free coatings can be obtained at 532 and 473 nm). The efficiency order is in line with the amount of light absorbed by this

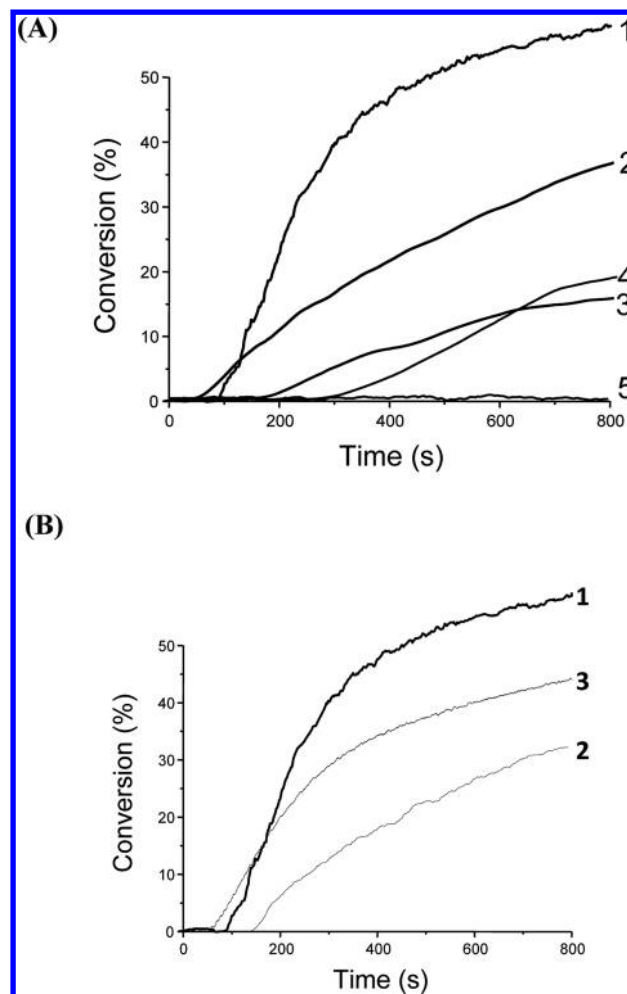


**Figure 4.** Photopolymerization profiles of EPOX under air. (A) Upon a laser diode, exposure at 532 nm in the presence of (1) **M\_1**/NVK/Iod (0.3%/3%/2% w/w), (2) **M\_3**/NVK/Iod (0.3%/3%/2% w/w), (3) **M\_2**/NVK/Iod (0.3%/3%/2% w/w), (4) **M\_5**/NVK/Iod (0.3%/3%/2% w/w), and (5) **M\_6**/NVK/Iod (0.3%/3%/2% w/w). (B) In the presence of **M\_1**/NVK/Iod (0.3%/3%/2% w/w) using different laser diode irradiations: (1) 532 nm; (2) 457 nm; (3) 473 nm.

compound at the laser line (457 < 473 < 532 nm). Interestingly, the **M\_1**/Iod/NVK can also be highly effective for the polymerization upon very low intensity sources: (i) green LED bulb exposure (a final conversion of ~55% can be reached after 30 min of irradiation), (ii) halogen lamp exposure (Figure S1 in the Supporting Information), or (iii) 405 nm laser diode exposure. Excellent polymerization profiles were also obtained for these soft irradiations conditions for the **M\_1**/Iod/(TMS)<sub>3</sub>Si–H initiating system. Interestingly, the **M\_1**/Iod/NVK system is also able to initiate the polymerization of Triethylene glycol divinyl ether (DVE-3) for these low intensities sources i.e. > 90% of conversion for 10 min of irradiation with green LED bulb or halogen lamp.

**3. Free Radical Photopolymerization.** The best typical conversion–time profiles of trimethylolpropane triacrylate (TMPTA) in laminated conditions under, e.g., a laser diode irradiation at 532 nm are shown in Figure 5. A quite slow conversion is obtained when using the **M\_1** (to **M\_6**)/MDEA (Figure 5 curve 1) or **M\_1** (to **M\_6**)/R–Br photoinitiating systems whereas a very fast rate of polymerization and relatively high conversions are reached with the three-component system

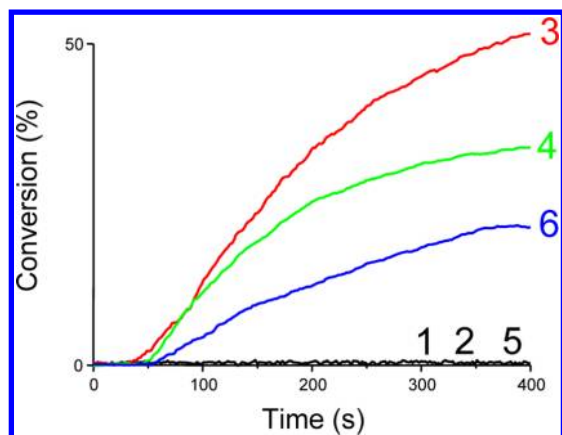
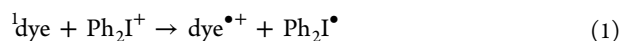
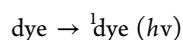


**Figure 5.** Photopolymerization profiles of TMPTA in laminated conditions upon a laser diode exposure at 532 nm in the presence of (1)  $M_1$ /MDEA (0.3%/4% w/w), (2)  $M_1$ /R-Br (0.3%/3% w/w), (3)  $M_1$ /MDEA/R-Br (0.3%/4%/3% w/w), (4)  $M_2$ /MDEA/R-Br (0.3%/4%/3% w/w), (5)  $M_3$ /MDEA/R-Br (0.3%/4%/3% w/w), and (6)  $M_4$ /MDEA/R-Br (0.3%/4%/3% w/w).

( $M_1$ /MDEA/R-Br; Figure 5 curve 3; final tack-free coatings within 10 min). The efficiency of the three-component systems decreases in the series  $M_1 > M_2 > M_4 > M_3 \sim M_5 \sim M_6$ .

**4. Chemical Mechanisms.** *a. The Dye/Iod/NVK for Cationic Polymerization.* When exposed to the laser diode at 532 nm, a very fast bleaching of the  $M_1$ /Iod solution is found (Figure 6). It results from the oxidation of  $M_1$  by Iod leading

(1–2) to  $PhI$ , ( $M_1$ ) $^{•+}$  and a phenyl radical  $Ph^{\bullet}$  as supported by ESR-ST and ESR experiments.  $Ph^{\bullet}$  (Figure 7A) and  $M_1^{\bullet+}$  (Figure 7B) are clearly observed: the hyperfine coupling constants  $hfc$  ( $a_N = 14.2$  G;  $a_H = 2.2$  G) agree with the known data for the PBN/ $Ph^{\bullet}$  adduct;<sup>18,21</sup> the radical cation is characterized by a distinct singlet signal with  $g \sim 2.003$  in agreement with.<sup>22</sup> Upon identical light absorbed intensities, the photolysis of the dye decreases in the series  $M_1 > M_3 > M_2 \sim M_5$  ( $M_4$ /Iod is not stable; see above;  $M_6$  has not been investigated i.e. this compound does not absorb at 532 nm) in the same way as the polymerization efficiency, thereby highlighting the role of the dye/Iod interaction in the global efficiency of the processes. Upon photolysis of dye/Iod solutions, a new product can be observed at about 650 nm; based on the ESR data, this absorption can be potentially ascribed to  $dye^{\bullet+}$  (see below). For the dye/Iod systems,  $dye^{\bullet+}$  corresponds to the initiating species for cationic polymerization of epoxides.



The free energy change  $\Delta G_{et}$  for the  ${}^1dye/Ph_2I^+$  electron transfer reaction is favorable according to the redox properties of the reactants (Table 2) (e.g.,  $E_{ox} = 0.75$  V for  $M_1$  [from this work; see Figure 8A];  $E_{red}(Ph_2I^+) \sim -0.2$  V;<sup>1</sup>  $E(M_1) \sim 2.15$  eV (Figure 8B; from the crossing of fluorescence and absorption spectra)). In laser flash photolysis experiments, no

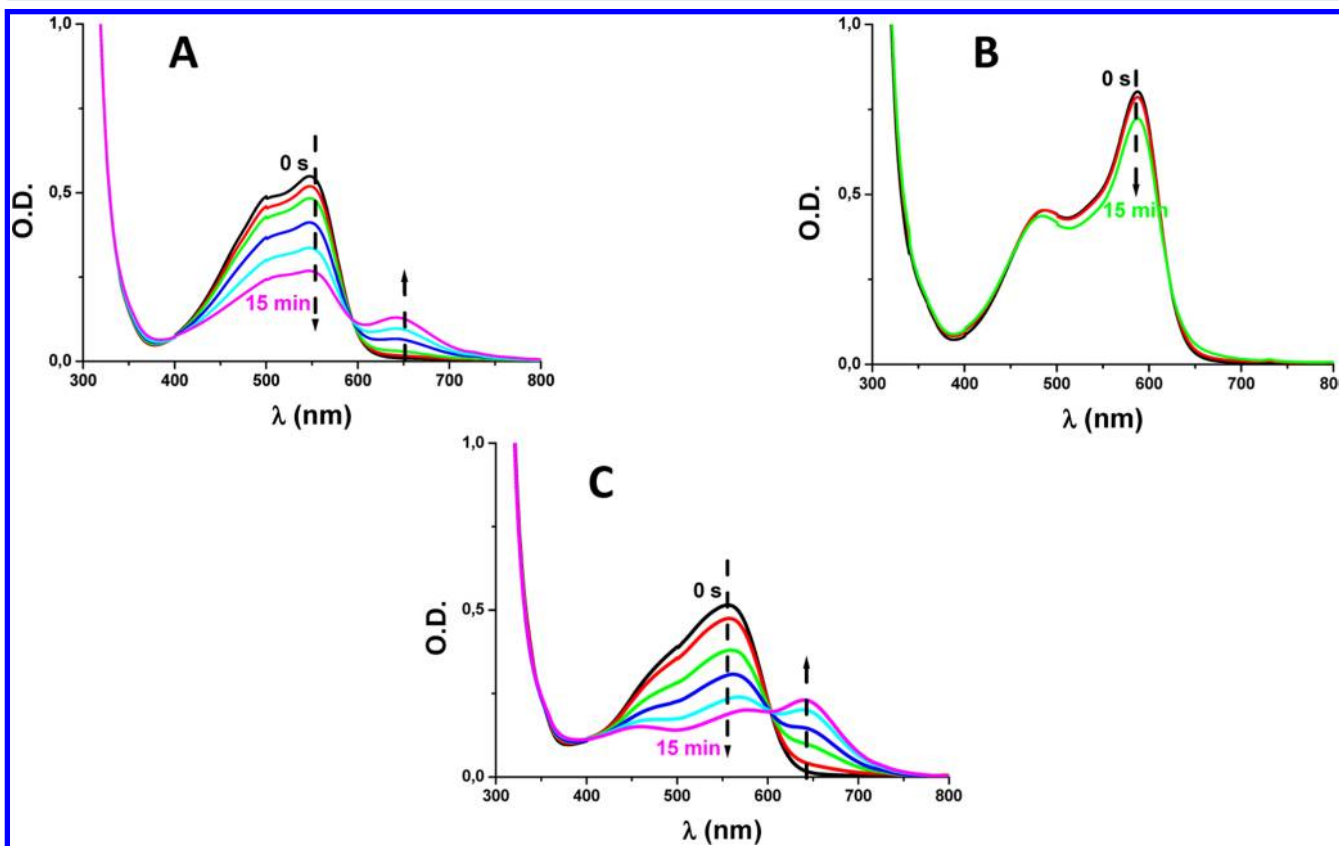


**Figure 6.** Photolysis of  $M_1$ /Iod (A),  $M_2$ /Iod (B), and  $M_3$ /Iod (C) in acetonitrile, under air, with a laser diode exposure at 532 nm (identical light absorption intensity).  $[Iod] = 0.011$  M; the UV–visible spectra are recorded at the same irradiation times.

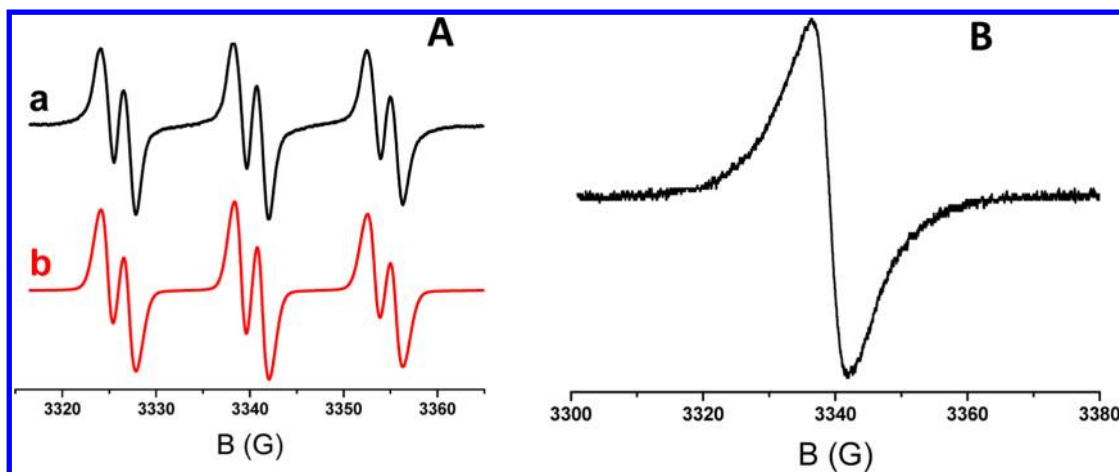


**Figure 7.** (A) ESR–spin trapping spectrum of  $M_1/Iod$ ;  $[Iod] = 0.01$  M. (B) ESR spectrum of the cation radical  $(M_1)^{\bullet+}$  at room temperature; in *tert*-butylbenzene; laser diode exposure at 532 nm; under  $N_2$ ; experimental (a) and simulated (b) spectra. Phenyl-*N-tert*-butylnitron (PBN) is used as spin trap in part A.

**Table 2. First Excited Singlet State Energy and Oxidation Potentials  $E_{ox}$  of  $M_1$  to  $M_6$ <sup>a</sup>**

	$\lambda_{abs}$ (nm)	$E_{S1}$ (eV)	$E_{ox}$ (SCE) (V)	$\Delta G_{et}$ (eV)
$M_1$	548	2.15	0.75	-1.2
$M_2$	586	2.01	0.8	-1.01
$M_3$	556	2.13	0.5	-1.43
$M_4$	476	–	–	<i>b</i>
$M_5$	491	2.46	0.8	-1.46
$M_6$	385	2.81	0.75	-1.86

<sup>a</sup>Free energy changes  $\Delta G_{et}$  of the  $M_1$  (to  $M_6$ )/Iod interaction; in acetonitrile. <sup>b</sup>Not stable in presence of Iod.

transient ascribable to a triplet state can be observed for  $M_1$  which is the most reactive dye: this confirms the  $S_1$  pathway (on the opposite, MK works in its triplet state). Reaction 1 being favorable for all the investigated dyes (see  $\Delta G_{et}$  Table 2), the lower photolysis found for different dye/Iod systems can be explained by a back electron transfer regenerating the starting compounds. Such a deactivation pathway decreases the yield in  $Ph^{\bullet}$  and  $dye^{\bullet+}$  in line with the very low efficiency of these systems in polymerization experiments (see above). Therefore, the relative efficiency of these dye/Iod combinations will be

affected by different parameters: (i) the relative dye light absorption properties, (ii) the radical or radical cation formation quantum yields in the singlet state and (iii) the ability of  $dye^{\bullet+}$  to initiate a ring-opening polymerization process.

As usually in presence of NVK,<sup>23</sup> the phenyl radicals ( $Ph^{\bullet}$ ) generated in eq 2 are easily converted into NVK $^{\bullet}$  by an addition to the double bond of NVK (eq 3). The formation of the NVK radicals (NVK $^{\bullet}$ ) upon irradiation of  $M_1/Ph_2I^+/NVK$  ( $a_N = 14.4$  G;  $a_H = 2.5$  G in agreement with<sup>18,23</sup>) is clearly observed in ESR spin trapping experiments. As previously discussed in other related systems,<sup>16b,24</sup> the NVK $^+$  cations are easily formed, i.e., NVK $^{\bullet}$  is an electron rich radical that can be easily oxidized (eqs 4a, 4b). These NVK $^+$  can very efficiently initiate the ROP of the epoxide (eq 5). Reaction 4b allows a partial regeneration of the dye as supported by photolysis experiments i.e. the photolysis of the dye in the three-component system (dye/Iod/NVK) is slower than in the two-component (dye/Iod) in agreement with 4b. The dye is only partially regenerated during the polymerization; i.e., the presence of radical cations inserted in the final polymer network is easily observed in ESR experiments (Figure S2 in the Supporting Information). These species are very stable and

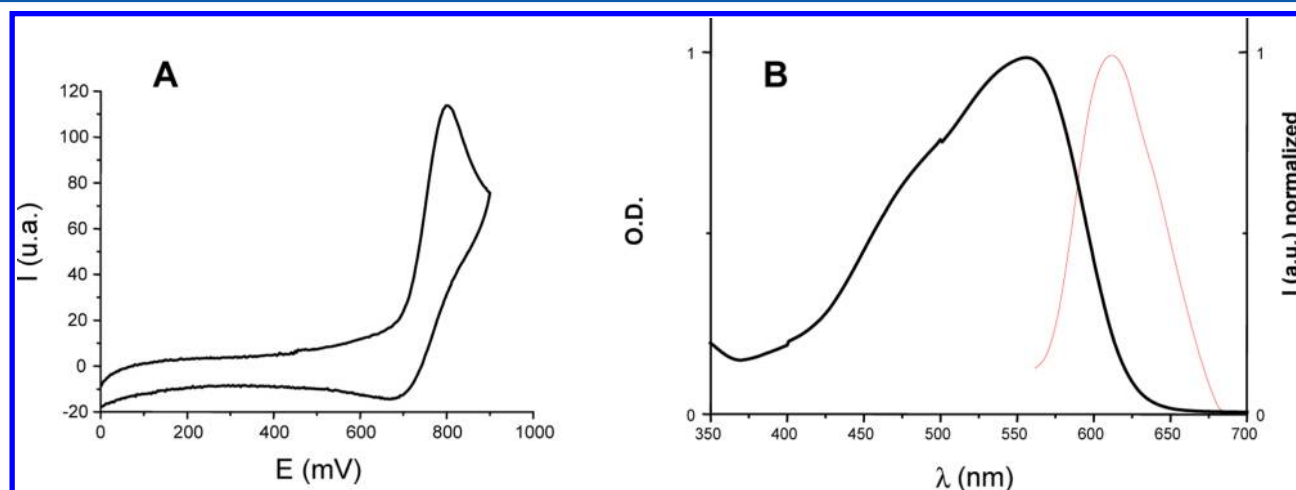


**Figure 8.** (A) Cyclic voltammogram of  $M_1$  in acetonitrile. (B) (a) Absorption and (b) fluorescence spectra of  $M_3$  in acetonitrile.

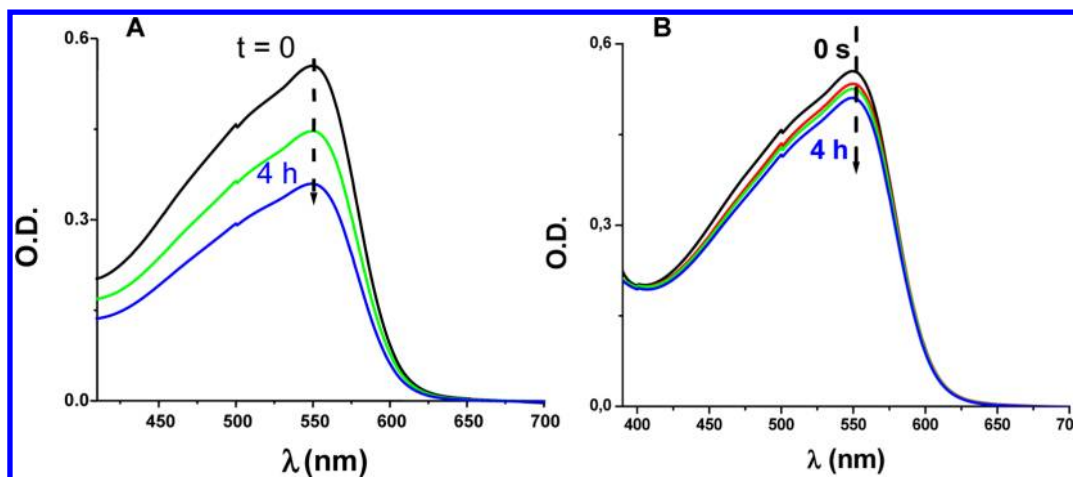


**Figure 9.** Photolysis of  $M_1$ /MDEA ( $[MDEA] = 0.25M$ ) (A);  $M_1$ /MDEA/R-Br ( $[MDEA] = 0.25M$ ;  $[R-Br] = 0.08M$ ) (B); in acetonitrile; under  $N_2$ ; low intensity laser diode exposure at 532 nm. Identical light absorption intensity.

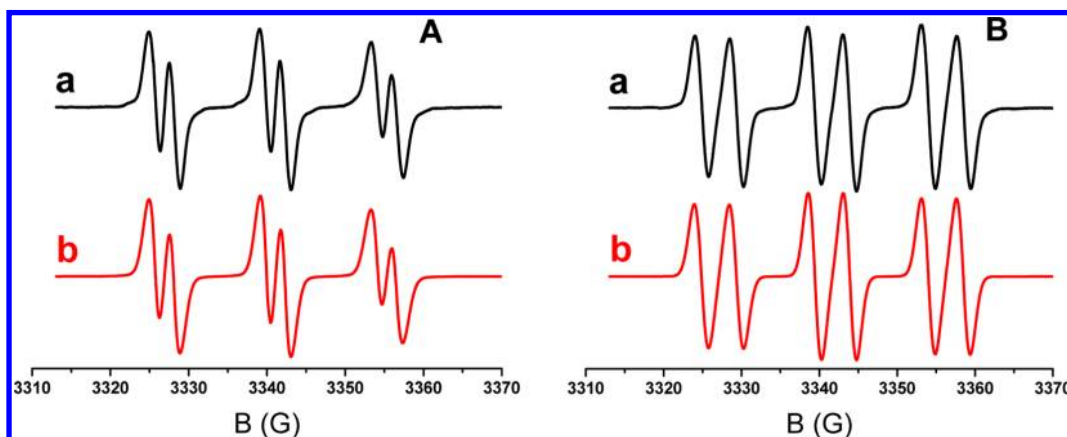
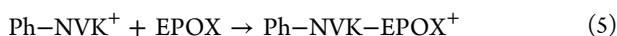


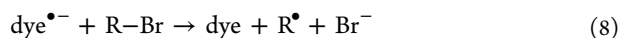
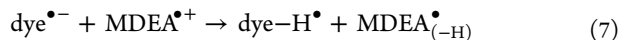
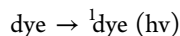
**Figure 10.** (A) ESR-spin trapping spectrum of  $M_1$ /ethylidimethylaminobenzoate (EDB); (B) ESR-Spin Trapping spectrum of  $M_1$ /(EDB)/phenacyl bromide (R-Br); laser diode exposure at 532 nm; experimental (a) and simulated (b) spectra. Phenyl-*N-tert*-butylnitron (PBN) is used as spin trap; under  $N_2$ .

persistent during several weeks. The investigation of the magnetic properties of these materials is beyond the scope of the present paper but can be worthwhile for different magnetism applications.



**b. Dye/Amine/Alkyl Halide for Free Radical Polymerization.** As above, a bleaching of the  $M_1$ /amine (MDEA) solution is found upon the laser diode exposure at 532 nm (Figure 9). It results (eq 6) from the reduction of  $M_1$  by MDEA leading to  $(M_1)^{\bullet-}$  and a subsequent proton transfer leading to aminoalkyl radical  $MDEA^{\bullet(-H)}$  (eq 7). This is supported by ESR-ST experiments; i.e., an aminoalkyl radical is clearly observed in an irradiated  $M_1$ /ethylidimethylaminobenzoate (EDB) solution: the hyperfine coupling constants  $hfc$  ( $a_N = 14.3$  G;  $a_H = 2.4$  G; Figure 10) agree with the known data for the PBN/aminoalkyl radical adduct;<sup>18</sup> EDB (instead of MDEA) is used to avoid a high polarity of the sample preventing an ESR analysis.

Remarkably, only phenacyl radicals ( $a_N = 14.9$  G;  $a_H = 4.6$  G) are observed in ESR-ST experiments upon the irradiation of the  $M_1$ /MDEA/R-Br three-component system (Figure 10B).<sup>25</sup> Their formation is explained on the basis of (6) and (8). As no aminoalkyls are detected, reaction 7 must be considered as unable to compete with (8). Interestingly, reaction 8 ensures a regeneration of the dye. This is fully consistent with the photolysis of  $M_1$ /MDEA/R-Br that is much slower than that of  $M_1$ /MDEA (Figure 9A vs Figure 9B). This behavior highlights a photocatalyst behavior for  $M_1$ . The phenacyl radicals initiate the FRP of TMPTA (9).



The relative efficiency of the dye/MDEA/R-Br combinations is rather complex and can be affected by different parameters: (i) the relative dye light absorption properties, (ii)

the radical or radical cation formation quantum yields and (iii) the rate constants for eqs 6 and 8.

## CONCLUSION

In this paper, we showed that bifunctional dyes derived from the Michler's ketone structure allow efficient radical polymerization of TMPTA and cationic polymerization of EPOX upon exposure to 405, 457, 473, and 532 nm laser diodes (100 mW/cm<sup>2</sup>) as well as to a green LED bulb at 514 nm or a halogen lamp. Five of these original dyes exhibit a unique push-pull molecular character which explains their remarkable red-shifted absorptions. Once again, it appeared that free radical promoted cationic polymerization (and obviously free radical polymerization) can be easily carried out under exposure to visible light sources. Other colored photoinitiators will be proposed in the future.

## ASSOCIATED CONTENT

### Supporting Information

Figure S1, photopolymerization profiles of EPOX under air upon a halogen lamp exposure in the presence of M<sub>1</sub>/Iod and M<sub>1</sub>/NVK/Iod; Figure S2, ESR spectrum for a polymer synthesized upon irradiation of EPOX at 532 nm (initiating system M<sub>1</sub>/Iod/NVK 0.3/2/3% w/w). This material is available free of charge via the Internet at <http://pubs.acs.org/>.

## AUTHOR INFORMATION

### Corresponding Author

\*E-mail: (J.L.) [jacques.lalevee@uha.fr](mailto:jacques.lalevee@uha.fr); (D.G.) [didier.gigmes@univ-amu.fr](mailto:didier.gigmes@univ-amu.fr).

### Notes

The authors declare no competing financial interest.

## ACKNOWLEDGMENTS

This work was partly supported by the "Agence Nationale de la Recherche" Grant ANR 2010-BLAN-0802. J.L. thanks the Institut Universitaire de France for the financial support.

## REFERENCES

- (1) Fouassier, J.-P.; Lalevée, J. *Photoinitiators for Polymer Synthesis: Scope, Reactivity and Efficiency*; Wiley-VCH: Weinheim, Germany, 2012.
- (2) (a) Dietliker, K. *A Compilation of Photoinitiators Commercially Available for UV Today*; Sita Technology Ltd.: Edinburgh and London, 2002; (b) Green, W. A.; *Industrial Photoinitiators*; CRC Press: Boca Raton, FL, 2010, (c) Allen, N. S.; *Photochemistry and Photophysics of Polymer Materials*; Wiley: New York, 2010; (d) *Photoinitiated Polymerization*, Belfied, K. D., Crivello, J. V., Eds.; ACS Symposium Series 847; American Chemical Society: Washington, DC, 2003.
- (3) Turro, N. J. *Modern Molecular Photochemistry*; University Science Books: New York, 1991.
- (4) (a) Schnabel, W. in *Lasers in Polymer Science and Technology*, Fouassier, J. P., Rabek, J. F., Eds.; CRC Press: Boca Raton, FL, 1990, Vol. II, pp 95–143; (b) Rullman, D.; Fouassier, J. P. *Eur. Polym. J.* **1991**, *27*, 991; *Eur. Polym. J.* **1992**, *28*, 591–597. (c) Fouassier, J. P. In *Radiation Curing in Polymer Science and Technology*; Fouassier, J. P., Rabek, J. F., Eds.; Elsevier: Barking, U.K., 1993; Vol. 1, pp 49–118; 1993, Vol. 2, pp 1–62; (d) Lissi, E. A., Encinas, M. V. In *Photochemistry and Photophysics*; Rabek, J. F., Ed.; CRC Press: Boca Raton, FL, 1991; Vol. 4, pp 221–293. (e) Wang, H.; Wei, J.; Jiang, X.; Yin, J. *Macromol. Chem. Phys.* **2006**, *207*, 1080–1086. (f) Nagarajan, R., Jr.; Bowers, J. S.; Wu, Z.; Cui, H.; Bao, R.; Jonsson, S.; McCartney, R., Jr.; Pittman, C. U.; Cao, L.; Ran, R. *Surf. Coat. Int.* **1999**, *82*, 344–

347. (g) Wang, H.; Shi, Y.; Wei, J.; Jiang, X.; Yin, J. *J. Appl. Polym. Sci.* **2006**, *101*, 2347–2354. (h) Tanaka, M.; Yago, T.; Wasaka, M. *Chem. Lett.* **2009**, *38*, 1086–1087. (i) Decker, C.; Moussa, K. *J. Polym. Sci., Polym. Lett.* **1989**, *27*, 347–354.

(5) (a) Green, W. A.; Timms, A. W. In *Radiation Curing in Polymer Science and Technology*; Fouassier, J. P., Rabek, J. F., Eds.; Elsevier: Barking, U.K., 1993; Vol. II, pp 375–434. (b) Fouassier, J. P., Loughnot, D. J. In *Lasers in Polymer Science and Technology*; Fouassier, J. P.; Rabek, J. F., Eds.; CRC Press: Boca Raton, FL, 1990; Vol. II, pp 145–168. (c) Corrales, T.; Catalina, F.; Allen, N. S.; Peinado, C. In *Photochemistry and UV Curing: new trends*; Fouassier, J. P., Ed.; Research Signpost: Trivandrum, India, 2006; pp 31–45. (d) Liska, R.; Knaus, S.; Gruber, H.; Wendrinsky, J. *Surf. Coat. Int.* **2000**, *83*, 297–303.

(6) (a) Neckers, D. C.; Valdes-Aguilera, O. M. In *Advances in Photochemistry*; Hammond, D. H., Gollnick, G. S.; Eds.; Wiley: New York, 1993. (b) Tasdelen, M. A.; Kumbaraci, V.; Talinli, N.; Yagci, Y. *Macromolecules* **2007**, *40*, 4406–4408. (c) Wang, K.; Ma, G.; Yin, R.; Nie, J.; Yu, Q. *Mater. Chem. Phys.* **2010**, *124*, 453–457. (d) Cui, R.; Wang, K.; Ma, G.; Qian, B.; Yang, J.; Ju, Q.; Nie, J. *J. Appl. Polym. Sci.* **2011**, *120*, 2754–2759. (e) Pietrzak, M.; Wrzyszczyński, A. *J. Appl. Polym. Sci.* **2011**, *122*, 2604–2608. (f) Yang, J.; Shi, S.; Xu, F.; Nie, J. *Photochem. Photobiol. Sci.* **2013**, *12*, 323–329.

(7) (a) Wang, Y.; Jiang, X.; Yin, J. *Eur. Polym. J.* **2009**, *45*, 437–447. (b) Wei, J.; Liu, F.; Lu, Z.; Song, L.; Cai, D. *Polym. Adv. Tech.* **2008**, *19*, 1763–1770. (c) Sun, F.; Zhang, N.; Nie, J.; Du, H. *J. Mater. Chem.* **2011**, *21*, 17290–17296. (d) Temel, G.; Aydogan, B.; Arsu, N.; Yagci, Y. *Macromolecules* **2009**, *42*, 6098–6106. (e) Allen, N. S. *J. Photochem. Photobiol. A* **1996**, *100*, 101–107. (f) Temel, G.; Aydogan, B.; Arsu, N.; Yagci, Y. *J. Polym. Sci., Part A: Polym. Chem.* **2009**, *47*, 2938–2947. (g) Wei, J.; Liu, F. *Macromolecules* **2009**, *42*, 5486–5491. (h) Pouliquen, L.; Coqueret, X.; Morlet-Savary, F.; Fouassier, J. P. *Macromolecules* **1995**, *28*, 8028–8034. (i) Matsushima, H.; Hait, S.; Li, Q.; Zhou, H.; Shirai, M.; Hoyle, C. E. *Eur. Polym. J.* **2010**, *46*, 1278–1287. (j) Chen, Y.; Loccufier, J.; Vanmaele, L.; Frey, H. *J. Mater. Chem.* **2007**, *17*, 3389–3392. (k) Wang, H.; Wei, J.; Jiang, X.; Yin, J. *J. Photochem. Photobiol. A: Chem.* **2007**, *186*, 106–114. (l) Sandholzer, M.; Schuster, M.; Liska, R.; Turecek, C.; Varga, F.; Stelzer, F.; Slugovc, C. *Polym. Prepr.* **2007**, *48*, 925–926. (m) Wei, J.; Wang, B. *Macromol. Chem. Phys.* **2011**, *212*, 88–95. (n) Wen, Y.; Jiang, X.; Yin, J. *Prog. Org. Coatings* **2009**, *66*, 65–72. (o) Xiao, P.; Dai, M.; Nie, J. *J. Appl. Polym. Sci.* **2008**, *108*, 665–670. (p) Xiao, P.; Zhang, H.; Dai, M.; Nie, J. *Prog. Org. Coatings* **2009**, *64*, 510–514. (q) Allen, N. S. *Photochemistry* **2007**, *36*, 232–297.

(8) (a) Li, Z.; Siklos, M.; Pucher, N.; Cicha, K.; Ajami, A.; Husinsky, W.; Rosspointner, A.; Vauthey, E.; Gescheidt, G.; Stampfl, J.; Liska, R. *J. Polym. Sci., Part A: Polym. Chem.* **2011**, *49*, 3688–3699. (b) Baldeck, P.; Stephan, O.; Andraud, C. In *Basics of Photopolymerization Reactions*; Fouassier, J. P., Allonas, X., Eds., Researchsignpost: Trivandrum, India, 2010; Vol. 3, pp 200–220.

(9) (a) Fouassier, J. P.; Loughnot, D. J.; Avar, L. *Polymer* **1995**, *36*, 5005–5010. (b) Morlet - Savary, F.; Fouassier, J. P.; Tomioka, H. *Polymer* **1992**, *33*, 4202–4206. (c) Fouassier, J. P.; Loughnot, D. *Polym. Commun.* **1990**, *31*, 417–422. (d) Allonas, X.; Lalevée, J.; Fouassier, J. P.; Visconti, M. *J. Polym. Sci., Part A: Polym. Chem.* **2000**, *38*, 4531–4541. (e) Lalevée, J.; Blanchard, N.; El Roz, M.; Graff, B.; Allonas, X.; Fouassier, J. P. *Macromolecules* **2008**, *41*, 4180–4186. (f) Guillaneuf, Y.; Bertin, D.; Gigmes, D.; Versace, D. L.; Lalevée, J.; Fouassier, J. P. *Macromolecules* **2010**, *43*, 2204–2212. (g) Griesser, M.; Dvorak, C.; Jauk, S.; Hofer, M.; Rosspointner, A.; Grabner, G.; Liska, R.; Gescheidt, G. *Macromolecules* **2012**, *45*, 1737–1745.

(10) (a) Lalevée, J.; Tehfe, M. A.; Dumur, F.; Gigmes, D.; Morlet-Savary, F.; Graff, B.; Fouassier, J. P. *Macromol. Rapid Commun.* **2013**, *34*, 239–245. (b) Tehfe, M. A.; Dumur, F.; Graff, B.; Clément, J. L.; Gigmes, D.; Morlet-Savary, F.; Fouassier, J. P.; Lalevée, J. *Macromolecules* **2013**, *46*, 736–746. (c) Tehfe, M. A.; Lalevée, J.; Telitel, S.; Contal, E.; Dumur, F.; Gigmes, D.; Bertin, D.; Nechab, M.; Graff, B.; Morlet-Savary, F.; Fouassier, J. P. *Macromolecules* **2012**, *45*, 4454–4460.

(11) Tehfe, M.-A.; Dumur, F.; Graff, B.; Gigmes, D.; Fouassier, J.-P.; Lalevée, J. *Macromolecules* **2013**, DOI: ma-2013-005082.

(12) Mayr, H.; Ofial, A. R.; Sauer, J.; Schmied, B. *Eur. J. Org. Chem.* **2000**, *11*, 2013–2020.

(13) Dumur, F.; Mayer, C.; Dumas, R. E.; Míomandre, F.; Frigoli, M.; Sécheresse, F. *Org. Lett.* **2008**, *10*, 321–324.

(14) Boger, D. L.; Wysocki, R. J., Jr. *J. Org. Chem.* **1988**, *53*, 3408–3421.

(15) (a) Tehfe, M. A.; Lalevée, J.; Dumur, F.; Zein-Fakih, A.; Telitel, S.; Gigmes, D.; Contal, E.; Bertin, D.; Morlet-Savary, F.; Graff, B.; Fouassier, J. P. *Eur. Polym. J.* **2013**, DOI: 10.1016/j.eurpolymj.2013.01.023. (b) Tehfe, M. A.; Lalevée, J.; Morlet-Savary, F.; Graff, B.; Blanchard, N.; Fouassier, J. P. *Macromolecules* **2012**, *45*, 1746–1752.

(16) (a) Lalevée, J.; Tehfe, M. A.; Gigmes, D.; Fouassier, J. P. *Macromolecules* **2010**, *43*, 6608–6615. (b) Lalevée, J.; Tehfe, M. A.; Zein-Fakih, A.; Ball, B.; Telitel, S.; Morlet-Savary, F.; Graff, B.; Fouassier, J. P. *ACS Macro Lett.* **2012**, *1*, 802–806.

(17) (a) Frisch, M. J.; Trucks, G. W.; Schlegel, H. B.; Scuseria, G. E.; Robb, M. A.; Cheeseman, J. R.; Zakrzewski, V. G.; Montgomery, J. A.; Stratmann, R. E. J.; Burant, C.; Dapprich, S.; Millam, J. M.; Daniels, A. D.; Kudin, K. N.; Strain, M. C.; Farkas, O.; Tomasi, J.; Barone, V.; Cossi, M.; Cammi, R.; Mennucci, B.; Pomelli, C.; Adamo, C.; Clifford, S.; Ochterski, J.; Petersson, G. A.; Ayala, P. Y.; Cui, Q.; Morokuma, K.; Salvador, P.; Dannenberg, J. J.; Malick, D. K.; Rabuck, A. D.; Raghavachari, K.; Foresman, J. B.; Cioslowski, J.; Ortiz, J. V.; Baboul, A. G.; Stefanov, B. B.; Liu, G.; Liashenko, A.; Piskorz, P.; Komaromi, I.; Gomperts, R.; Martin, R. L.; Fox, D. J.; Keith, T.; Al-Laham, M. A.; Peng, C. Y.; Nanayakkara, A.; Challacombe, M.; Gill, P. M. W.; Johnson, B.; Chen, W.; Wong, M. W.; Andres, J. L.; Gonzalez, C.; Head-Gordon, M. E.; Replogle, S.; Pople, J. A. *Gaussian 03, Revision B-2*; Gaussian, Inc.: Pittsburgh, PA, 2003. (b) Foresman, J. B.; Frisch, A. *Exploring Chemistry with Electronic Structure Methods*; 2nd ed., Gaussian, Inc.: Pittsburgh, PA, 1996.

(18) (a) Tordo, P. *Spin-trapping: recent developments and applications*; Atherton, N. M., Davies, M. J., Gilbert, B. C., Eds.; Electron Spin Resonance 16; The Royal Society of Chemistry: Cambridge, U.K., 1998. (b) Landolt Bornstein: *Magnetic Properties of Free Radicals*; Fischer, H., Ed.; Springer Verlag: Berlin, 2005; Vol. 26d. (c) Chandra, H.; Davidson, I. M. T.; Symons, M. C. R. *J. Chem. Soc. Faraday Trans. 1* **1983**, *79*, 2705–2711. (d) Alberti, A.; Leardini, R.; Pedulli, G. F.; Tundo, A.; Zanardi, G. *Gazz. Chim. Ital.* **1983**, *113*, 869–871.

(19) Rehm, D.; Weller, A. *Isr. J. Chem.* **1970**, *8*, 259–265.

(20) Lalevée, J.; Dirani, A.; El Roz, M.; Graff, B.; Allonas, X.; Fouassier, J. P. *Macromolecules* **2008**, *41*, 2003–2010.

(21) Lalevée, J.; Blanchard, N.; Tehfe, M. A.; Morlet-Savary, F.; Fouassier, J. P. *Macromolecules* **2011**, *43*, 10191–10195.

(22) Kim, S. J.; Jang, H.-G.; Lee, J. K.; Min, H.-K.; Hong, S. B.; Seo, G. *Chem. Commun.* **2011**, *47*, 9498–9500.

(23) Lalevée, J.; Dumur, F.; Mayer, C. R.; Gigmes, D.; Nase, G.; Tehfe, M. A.; Telitel, S.; Morlet-Savary, F.; Graff, B.; Fouassier, J. P. *Macromolecules* **2012**, *45*, 4134–4141.

(24) Hua, Y.; Crivello, J. V. *J. Polym. Sci., Part A: Polym. Chem.* **2000**, *38*, 3697–3709.

(25) Lalevée, J.; Tehfe, M. A.; Dumur, F.; Gigmes, D.; Blanchard, N.; Morlet-Savary, F.; Fouassier, J. P. *ACS Macro Lett* **2012**, *1*, 286–290.